MITSUBISHI ELECTRIC RESEARCH LABORATORIES
https://www.merl.com

Broken-bar Fault Detection by Injecting a Frequency Modulated Continuous Wave Signal

Liu, Dehong; Varatharajan, Anantaram; Goldsmith, Abraham; Kong, Chuizheng; Sigatapu, Laxman; Wang, Yebin

TR2023-039 May 16, 2023

Abstract

It is challenging to detect broken-bar faults in squirrel-cage induction motors using motor current signature analysis (MCSA) due to the small magnitude and proximity of the fault signature relative to the operating frequency component, especially when the motor slip is very small. In this paper we propose a signal injection method to detect the broken-bar fault by injecting a frequency modulated continuous wave (FMCW) signal to the stator voltage. Model analysis and simulation show that under broken-bar fault conditions, the injected FMCW signal induces another FMCW signal of a lower frequency band, which as a newly-defined fault signature can be extracted by analyzing cross correlation between the injected signal and the induced signal in the frequency domain. Compared to other signal injection methods, our method is more robust and insusceptible to harmonic interference. Experimental results on a three-phase squirrel-cage induction motor validate our method in detecting broken-bar faults from noisy measurements even when the motor slip is very small.

IEEE International Electric Machines and Drives Conference (IEMDC) 2023

Mitsubishi Electric Research Laboratories, Inc.
201 Broadway, Cambridge, Massachusetts 02139

Broken-bar Fault Detection by Injecting a Frequency Modulated Continuous Wave Signal

Dehong Liu
Mitsubishi Electric Research Labs
Cambridge, MA, USA
liudh@merl.com

Anantaram Varatharajan
Mitsubishi Electric Research Labs
Cambridge, MA, USA
varatharajan@merl.com

Abraham Goldsmith
Mitsubishi Electric Research Labs
Cambridge, MA, USA
goldsmith@merl.com

Chuizheng Kong*
Rensselaer Polytechnic Institute
Troy, NY, USA
kongc2@rpi.edu

Laxman Kumar Sigatapu*
Northeastern University
Boston, MA, USA
sigatapu.l@northeastern.edu

Yebin Wang
Mitsubishi Electric Research Labs
Cambridge, MA, USA
yebinwang@ieee.org

***Abstract*—It is challenging to detect broken-bar faults in squirrel-cage induction motors using motor current signature analysis (MCSA) due to the small magnitude and proximity of the fault signature relative to the operating frequency component, especially when the motor slip is very small. In this paper we propose a signal injection method to detect the broken-bar fault by injecting a frequency modulated continuous wave (FMCW) signal to the stator voltage. Model analysis and simulation show that under broken-bar fault conditions, the injected FMCW signal induces another FMCW signal of a lower frequency band, which as a newly-defined fault signature can be extracted by analyzing cross correlation between the injected signal and the induced signal in the frequency domain. Compared to other signal injection methods, our method is more robust and insusceptible to harmonic interference. Experimental results on a three-phase squirrel-cage induction motor validate our method in detecting broken-bar faults from noisy measurements even when the motor slip is very small.**

***Index Terms*—Broken-bar, Fault detection, Induction motor, Signal injection, FMCW**

I. Introduction

Broken bar is one of the most common faults in squirrel-cage induction motors [1]. Although the broken-bar fault does not incur an instant failure to the induction motor in general, it causes serious secondary effects such as poor starting performance, excessive vibration, and torque fluctuation, *etc*. In some situations, the broken piece may hit stator windings at high velocity, damaging the winding insulation. Therefore, it is of great importance to detect the broken-bar fault and have a timely maintenance [2].

To detect the broken-bar fault, the motor current signature analysis (MCSA)-based method is widely used for its non-invasiveness and low cost. When one or more rotor bars were broken in the squirrel-cage induction motor, the asymmetric rotor will induce frequency components $f_b = (1 \pm 2\kappa s) f_0$ in the stator current [3] during rotating operation, where f_0 is the power supply frequency; s is the speed slip; and κ is the harmonic frequency index. Among these extra components, the component $(1 - 2s) f_0$ is the strongest one and typically treated as the characteristic frequency of a broken-bar fault. Therefore, broken-bar fault detection using the MCSA-based method is achieved by detecting the characteristic frequency component $(1 - 2s) f_0$.

In practice, there are three issues in detecting the characteristic frequency component. First, the magnitude of the characteristic frequency is relatively small, depending on the total number of rotor bars. For example, for a 30-rotor bar squirrel-cage motor, the fault component is typically $30 \sim 40dB$ lower than that of the fundamental power supply frequency component. The more the number of rotor bars, the lower the relative magnitude of fault components. Second, the characteristic frequency is very close the power supply frequency f_0. Under steady operating condition the speed slip typically ranges from 0.005 to 0.05. For $f_0 = 50$Hz power supply, the difference between the characteristic frequency and the fundamental frequency f_0 can be as small as $0.01 f_0 = 0.5$Hz, making it difficult to discriminate the fault signature from the dominant operating frequency component. Third, the background noise interferes the detection performance. Because of these practical issues, the characteristic frequency can be submerged in the sidelobe of the fundamental frequency component or noise.

In the past decades, researchers have developed a variety of MCSA-based methods including signal injection to improve the detection performance. For example, advanced signal processing techniques such as ESPRIT [4], MUSIC [5], and compressive sensing [6] are utilized to achieve high resolution frequency spectrum such that the characteristic frequency component can be well separated. These methods typically require high signal-to-noise ratios and may perform poorly in strong noise conditions. For another example, researchers make use of the starting process of the motor to detect the broken-bar fault. When the motor speed is increasing from zero to the steady asynchronous speed, the speed slip s is decreasing from 1 to a small number close to 0. In this situation, the characteristic

*Chuizheng Kong and Laxman Kumar Sigatapu contributed on the experimental platform when they were interns at MERL.

frequency component is well separated with the fundamental frequency component in the frequency domain. However, this method requires a restart of the motor, which is not suitable for continuously operating motors and not preferred for online monitoring. The characteristic frequency also varies during the starting process, making it difficult to capture the fault characteristic frequency component in a short time.

In this paper, we proposed a signal injection method to detect motor broken-bar faults. In particular, a frequency modulated continuous wave (FMCW) signal is injected to the operating stator voltage, and then the stator current, which may or may not include induced fault signature, is measured for further analysis. This FMCW signal is of a small magnitude and a frequency band higher than the operating frequency. Since the magnitude is small, it will not interfere the operation of the motor. As the injected signal frequency band is higher than the operating frequency, the motor speed, which is a slightly lower than the synchronous speed of the operating frequency, becomes much lower than the synchronous speed of the injected signal. Consequently, this injected voltage signal will induce another FMCW signal in the stator current with a frequency band well separated from that of the injected signal if there exists a broken-bar fault. By analyzing the coherence between the induced current signal and the injected voltage signal using signal processing techniques, fault signature can be extracted robustly even under noisy conditions.

Comparing to existing signal injection methods [7]–[9], our proposed method is different from three aspects. First, our injected signal is a FMCW signal, which is different from a single high frequency signal or a narrow time-domain pulse used in other signal injection methods. Second, our fault signature is newly defined and extracted based on physical model and signal coherence analysis, not simply by thresholding a frequency component. Third, our method exhibits robust performance under noisy background, especially rich harmonic environments. To verify our method, a dynamic model of a squirrel cage induction motor is built, using a multi-loop equivalent circuit to represent the coupling between the stator and the rotor. Stator currents under healthy and faulty conditions are simulated respectively by changing the corresponding equivalent circuit. A newly defined fault signature is then extracted using signal processing techniques. Experimental results on a three-phase squirrel-cage induction motor also demonstrate that our method can effectively extract broken-bar fault signature even with very small slip and under strong-noise conditions.

This paper is organized as follows. In Section II we introduce the dynamic model of a squirrel-cage induction motor under healthy and faulty conditions. In Section III we analyze the fault signature in the stator current with FMCW signal injection. Simulation and experimental results are shown in Section IV, followed by conclusion drawn in Section V.

II. Dynamic Model of Induction Motor

In squirrel-cage induction motors, the stator consists of distributed windings of three phases, displaced by 120° spatial angle. The rotor contains longitudinal conductive bars connected at both ends by shorting rings, forming a squirrel-cage like shape. When the induction motor is operating, the stator windings set up a rotating magnetic field through the rotor, inducing electrical current in the rotor bars, producing force acting at a tangent orthogonal to the rotor, and resulting in torque to turn the shaft.

In the following part of this section, we first develop a dynamic model for motors in normal healthy conditions, then extend it to fault conditions. For simplicity, we neglect magnetic saturation and assume linear magnetic characteristics. We use bold capital letters for matrices, regular capital letters for constant parameters, and small letters for time-variant parameters.

Consider a squirrel-cage induction motor with n rotor bars. The equivalent circuit of squirrel-cage induction motor can then be modeled as $(n+1)$ independent current loops, where n of them are identical circuit loops under ideal condition, with each loop consisting of two adjacent rotor bars connected by two end ring portions. The remaining circuit loop is formed by one of the end rings. So, the current distribution in rotor can be specified in terms of $(n+1)$ independent loop currents, *i.e.*, n rotor-bar loop currents i_j $(1 \leq j \leq n)$ plus one end-ring loop current i_e.

A. Dynamic model of healthy condition

Based on the equivalent circuit, the voltage and flux linkage equations for the stator and the rotor can be written as

$$\mathbf{U}_s = \mathbf{R}_s\mathbf{I}_s + \frac{d\mathbf{\Psi}_s}{dt}, \tag{1}$$

$$\mathbf{\Psi}_s = \mathbf{L}_s\mathbf{I}_s + \mathbf{M}_{sr}\mathbf{I}_r, \tag{2}$$

$$\mathbf{U}_r = \mathbf{R}_r\mathbf{I}_r + \frac{d\mathbf{\Psi}_r}{dt}, \tag{3}$$

$$\mathbf{\Psi}_r = \mathbf{L}_r\mathbf{I}_r + \mathbf{M}_{rs}\mathbf{I}_s, \tag{4}$$

where $\mathbf{U}_s$, $\mathbf{I}_s$, $\mathbf{\Psi}_s$, $\mathbf{R}_s$, and $\mathbf{L}_s$ are the stator voltage, the stator current, the stator winding flux, the stator resistance, and the stator inductance, respectively; $\mathbf{U}_r$, $\mathbf{I}_r$, $\mathbf{\Psi}_r$, $\mathbf{R}_r$, and $\mathbf{L}_r$ are the rotor voltage, the rotor current, the rotor flux, the rotor resistance, and the rotor inductance, respectively; and $\mathbf{M}_{rs} = \mathbf{M}_{sr}$ are the stator-rotor mutual inductance.

Note that the stator winding resistance and the stator inductance in are constant under our assumption, while the stator-rotor mutual inductance varies with the angular position of the rotor. This is because the mutual inductance is related to the relative position between the stator windings and the rotor bars, which changes during operation. The mechanical equation of the induction motor can be expressed as

$$T_e - T_l = J\frac{d\omega_r}{dt}, \tag{5}$$

where T_e and T_l represent the electromagnetic torque and the mechanical load respectively, J stands for the rotor inertia, and ω_r is the angular velocity.

In summary, equations (1)$\sim$(5) form a dynamic model of induction motors with unknown stator and rotor currents.

Given motor parameters, initial conditions, stator voltages, and the load, we can solve initial value problem of differential equations to simulate the stator current during dynamic operation. Under normal healthy conditions, inductances and resistances in (1)∼(4) can be calculated [10], [11]. We skip the details of parameter calculations in this paper. Instead, we use public available parameters in our simulations.

B. Dynamic model of faulty condition

When one bar is fully broken, the related branch becomes open circuit. Then the total number of circuit loops is reduced by one since two related loops are replaced by a new loop with doubled end-ring segments, as shown in Fig. 1. Consequently, in (3)∼(4) the corresponding loops should be rebuilt with the equivalent parameters.

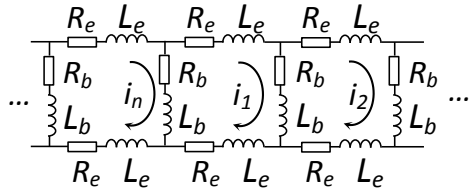

(a)

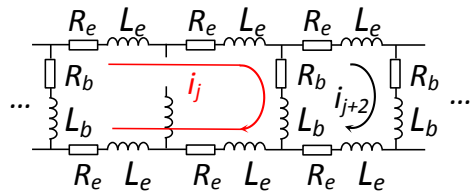

(b)

Fig. 1. Equivalent circuits of (a) a healthy rotor, and (b)a faulty rotor with one broken bar

III. FMCW Injection Based Broken-bar Fault Detection

In this section, we focus on fault signature extraction from signal processing perspective, ignoring details of hardware implementation. With an injected FMCW voltage signal on top of the original three-phase source voltage, the overall input voltage to the motor can be represented as follows

$$\begin{cases} u_a(t) = U_0\cos(2\pi f_0 t + \phi_0) + U_i\cos(\phi_a(t)), \\ u_b(t) = U_0\cos(2\pi f_0 t - 2\pi/3 + \phi_0) + U_i\cos(\phi_a(t) - 2\pi/3), \\ u_c(t) = U_0\cos(2\pi f_0 t + 2\pi/3 + \phi_0) + U_i\cos(\phi_a(t) + 2\pi/3), \end{cases} \tag{6}$$

where U_0 is the amplitude of the source voltage signal, U_i is the amplitude of the injected FMCW signal, and $\phi_a(t)$ is the phase angle of the injected FMCW signal in phase A. The three phase voltage source is balanced at any time with $2\pi/3$ phase difference.

The amplitude U_i is chosen to be small such that the injected signal barely interferes the motor operation, albeit is large enough such that the induced signal can be detected.

For phase $\phi_a(t)$, we consider a frequency sweep period of T. The phase can be expressed as [12]

$$\phi_a(t) = 2\pi(u(t)f_1 + f_2)t', \tag{7}$$

where f_1 and f_2 are two frequency parameters, and

$$u(t) = 2[\frac{t}{T} - \lfloor\frac{t}{T}\rfloor] - 1, \tag{8}$$

is a saw-tooth signal of period T whose magnitude increases from -1 at $t = 0$ to 1 at $t = T$; $\lfloor\cdot\rfloor$ is the floor function that gives the greatest integer less than the input real number as output; and t' is the frequency sweep time, which is also a saw-tooth signal of period T synchronized with $u(t)$ as

$$t' = t - \lfloor\frac{t}{T}\rfloor T = \frac{u(t)+1}{2}T. \tag{9}$$

From (7)∼(9) we have

$$\phi_a(t) = \phi_a(t+T). \tag{10}$$

The modulation frequency can be formulated as

$$\begin{aligned} f_M(t) &= \frac{1}{2\pi}\frac{\partial\phi_a}{\partial t} = 2u(t)f_1 + f_1 + f_2 \\ &\in [f_2 - f_1, f_2 + 3f_1] \end{aligned} \tag{11}$$

Given the modulation frequency range $[f_{min}, f_{max}] = [f_2 - f_1, f_2 + 3f_1]$, it is straightforward to calculate f_1 and f_2. It is worth noting that when $f_1 = 0$, the injected signal becomes a single frequency signal of frequency f_2. However, if f_1 is too large, meaning the bandwidth of the injected signal is too large, the induced signal may be overlapped with the injected signal in the frequency domain, making the fault signature extract more difficult. To determine the frequency range of the injected FMCW signal, we first examine the induced signal of a single high frequency injection of k^{th} harmonic without loss of generality. Given the motor speed n, the motor slip is calculated as

$$s = \frac{n_s - n}{n_s}. \tag{12}$$

If we treat the k^{th} harmonic as the virtual operating frequency, then the virtual motor slip is

$$s^k = \frac{n_s^k - n}{n_s^k} = \frac{kn_s - n}{kn_s}. \tag{13}$$

Since the amplitude of the injected k^{th} harmonic voltage is small, the motor will be driven by the fundamental frequency component with a steady low speed.

As aforementioned, under broken-bar fault condition, fault frequency components $f_b = (1 \pm 2\kappa s)f_0$ will be induced in the stator current, in which the dominant one is $(1 - 2s)f_0$. Similarly, the induced fault characteristic frequency component by the injected k^{th} harmonic in the motor current can be expressed as

$$(1 - 2s^k)f^k = (1 - 2\frac{kn_s - n}{kn_s})kf_0 = -[kf_0 - 2(1-s)f_0]. \tag{14}$$

It is observed from (14) that the absolute value of the induced frequency is $2(1-s)f_0$ lower than the injected frequency kf_0. Note that this frequency shift $2(1-s)f_0$ between the

injected signal and the induced signal is independent from the frequency of injection. Therefore, an injected signal with modulating frequency range $f \in [kf_0, (k+2(1-s))f_0]$ will induce a signal of frequency range of $[(k_0-2(1-s))f_0, kf_0]$. Although the magnitude of the induced signal by a single frequency component may be very small, the detection performance can be improved by combining all modulation frequency components. Following this idea, we compute the cross correlation between the injected signal $U_{ia}(f)$ and the stator current $I_{af}(f)$ as

$$R_{U_{ia},I_{af}}(f_d) = \sum_f U_{ia}(f+f_d)I^*_{af}(f). \tag{15}$$

If there exists an induced signal in the stator current similar to the injected signal, a spike in the cross-correlation function will appear at frequency $-2(1-s)f_0$. As a result, we can treat this spike as a newly defined fault signature, or an indicator of broken-bar fault if its magnitude is greater than a certain level, and vice versa. Since the fault signature is an integration effect of a signal with a certain frequency bandwidth, it is insusceptible to harmonics and other interference.

IV. Results

A. Simulations

To verify our proposed FMCW signal injection-based method for broken-bar fault detection, we simulate the stator current of a 1.5kW three-phase squirrel-cage induction motor under a broken-bar fault condition using the dynamic model presented in Section II. The model parameters [6] are listed in Table I. A balanced three-phase FMCW voltage signal of $[250\text{Hz}, 330\text{Hz}]$ (or $k = 5^{th} \sim 6.6^{th}$ harmonics) with 15% rated magnitude was injected to the power voltage source.

TABLE I
Motor parameters

n	$f_s(Hz)$	$R_s(\Omega)$	$R_e(\mu\Omega)$	$R_b(\mu\Omega)$
29	50	3.43	37	133.4
$L_s(H)$	$L_r(mH)$	$L_b(\mu H)$	$L_e(\mu H)$	$J(kg\cdot m^2)$
0.51563	5.443	1.08	0.01	0.0014

We show in Fig. 2 (a) the time-domain stator current when a FMCW voltage signal is injected to the power source. Its frequency spectrum is presented in Fig. 2(b). We notice that some frequency components in the range of $[150\text{Hz}, 230\text{Hz}]$ are induced. To extract the fault signature by analyzing the induced signal, we compute the cross correlation between the current frequency spectrum in Fig. 2(b) and the injected reference signal spectrum as shown in Fig.2 (c) using (15), with result shown in Fig.2 (d). Clearly a spike signal at frequency -100Hz appears as expected, indicating a broken-bar fault according to our analysis in Section III.

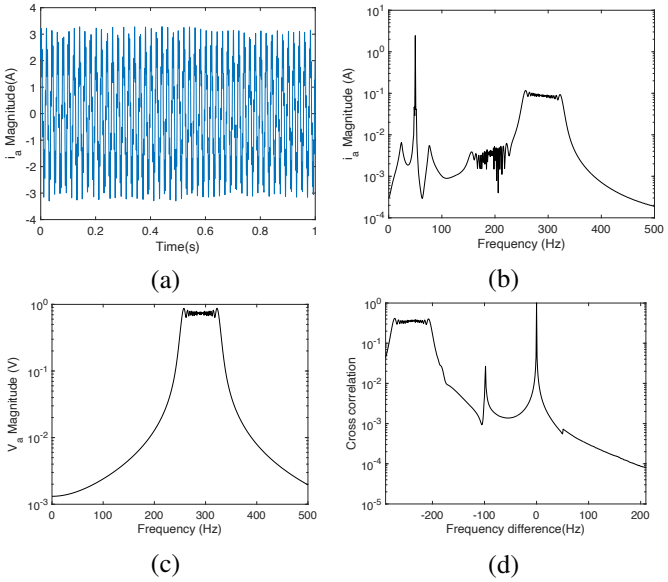

Fig. 2. Simulation results of (a)Time-domain stator current, (b)Frequency spectrum of stator current, (c)Spectrum of injected FMCW signal, and (d)Fault signature extraction by computing the cross-correlation between (b) and (c).

B. Experiments

To further demonstrate our method, we perform experiments on a 1HP three-phase squirrel-cage induction motor. The experimental setup is shown in Fig. 3 (a), where the motor is driven by a three-phase inverter, with gate PWM signals generated by a dSPACE® Scalexio Labbox platform. For comparison, we use two rotors of the same specifications, and manually produce a broken-bar fault on one of the two rotors by drilling a hole on a rotor bar. Pictures of the healthy rotor and the faulty rotor are shown in Fig. 3 (b) and (c) respectively.

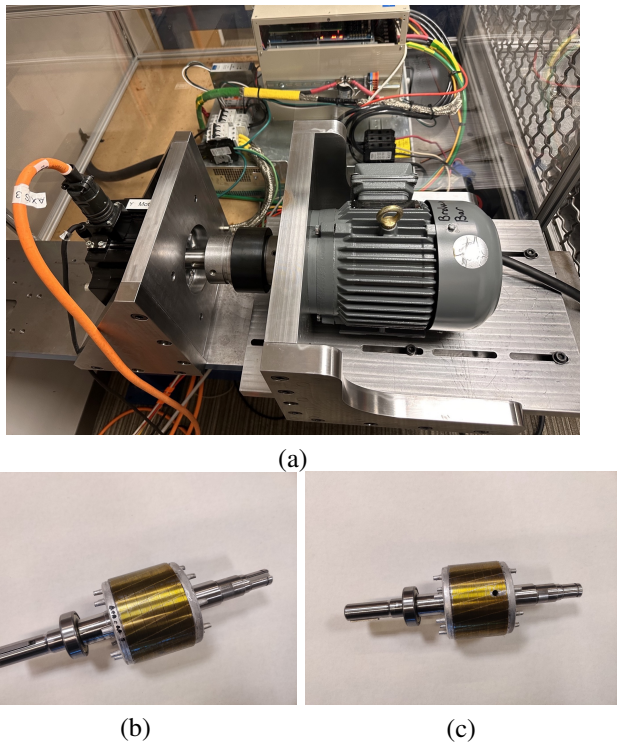

(a) (b) (c)

Fig. 3. (a) Experimental setup, (b) Healthy rotor, and (c) Faulty rotor.

We consider three methods to detect the broken-bar fault, including 1) MCSA without any signal injection, 2) MCSA with single frequency signal injection, and 3) our proposed method with FMCW signal injection.

1) No signal injection: The faulty motor is operating at a 50Hz power source and a light load condition with a speed of 1497rpm. Fig. 4 shows the frequency spectrum of stator current using MCSA. Since the motor speed is near the synchronous speed, the slip $s = 0.002$ is close to zero, conventional MCSA-based methods fail to extract the characteristic frequency component of broken-bar fault.

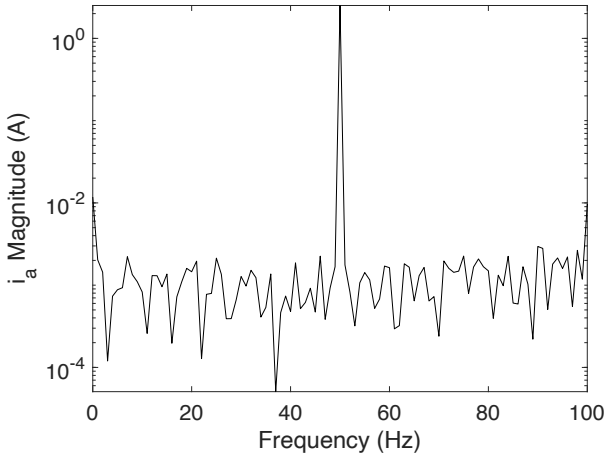

Fig. 4. Stator current spectrum of one-broken bar faulty condition when the slip is very small, in which the fault signature is not detectable.

2) Single frequency signal injection: During operation, a single-frequency signal of 275Hz is injected to the power voltage, as suggested by [7], [8], via the Scalexio platform, and the stator current is measured using a current sensor for further analysis and fault detection. In Fig. 5 we show the current frequency spectra of both healthy rotor and faulty rotor. From both spectra, we observe very rich harmonics. It is hard to tell which frequency component is corresponding to the fault signature.

3) FMCW signal injection: During operation, a small magnitude (approximately 15% of the rated voltage) FMCW voltage signal is injected to the power source via the Scalexio platform, with injected signal frequency band $[f_{min}, f_{max}] = [250, 330]$Hz, or $k = 5^{th} \sim 6.6^{th}$ harmonics. We show in Fig. 6(a) the time-domain voltage signal and in Fig. 6(b) the time-domain stator current signal. The frequency spectrum of the stator current of a faulty motor is shown in Fig. 6(c), and the cross correlation result between the stator current spectrum and the injected voltage signal is shown in Fig. 6(d). For comparison, we show the current spectrum of a healthy motor and its cross correlation analysis result in Fig. 6(e) and (f), respectively. It is clear that the fault signature appears at $f = -100$Hz for faulty motor as expected, and no fault signature for healthy motor. The experiment results agree with the simulation results presented in Fig. 2.

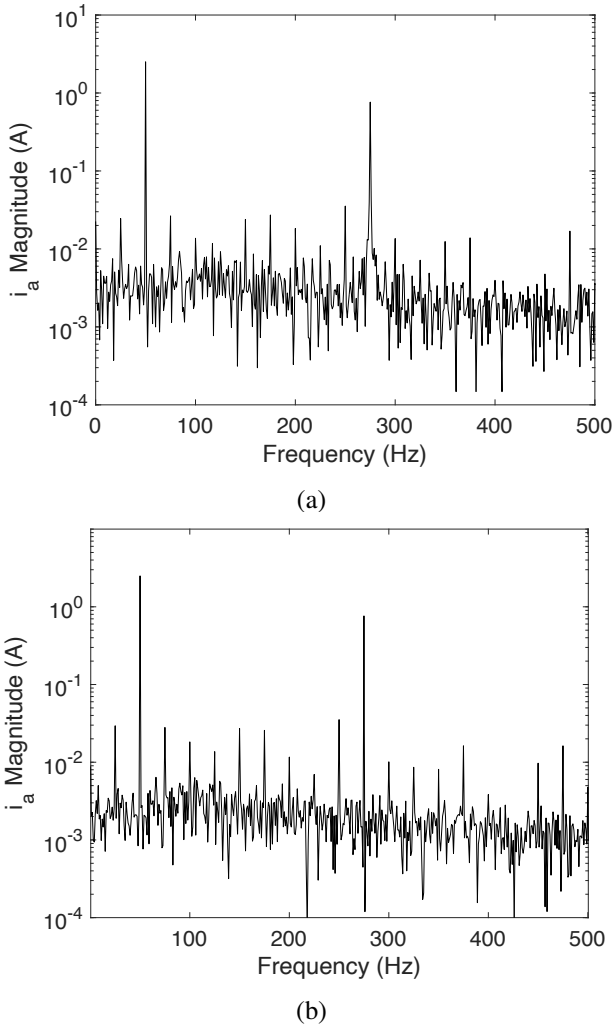

Fig. 5. Stator current spectrum with a single high frequency signal injection on (a) a healthy motor and (b) a broken-bar faulty motor. The fault signature is interfered by harmonics.

Compared to single frequency injection method, our proposed method can effectively extract fault signature from noisy measurements even under a very small slip. Our method is insusceptible to harmonics and other inference.

V. Conclusion

We proposed a broken-bar fault detection method to improve the detection performance by injecting a frequency modulated continuous wave (FMCW) voltage signal to the stator power source. Model analysis and simulation show that under broken-bar fault conditions, the injected FMCW signal induces another FMCW signal of a lower frequency band, which as a newly-defined fault signature can be extracted by analyzing cross correlation between the injected signal and the induced signal in the frequency domain. Simulation and experimental results demonstrate that our proposed method outperforms other methods in detecting broken-bar faults from noisy measurements when the motor slip is very small.

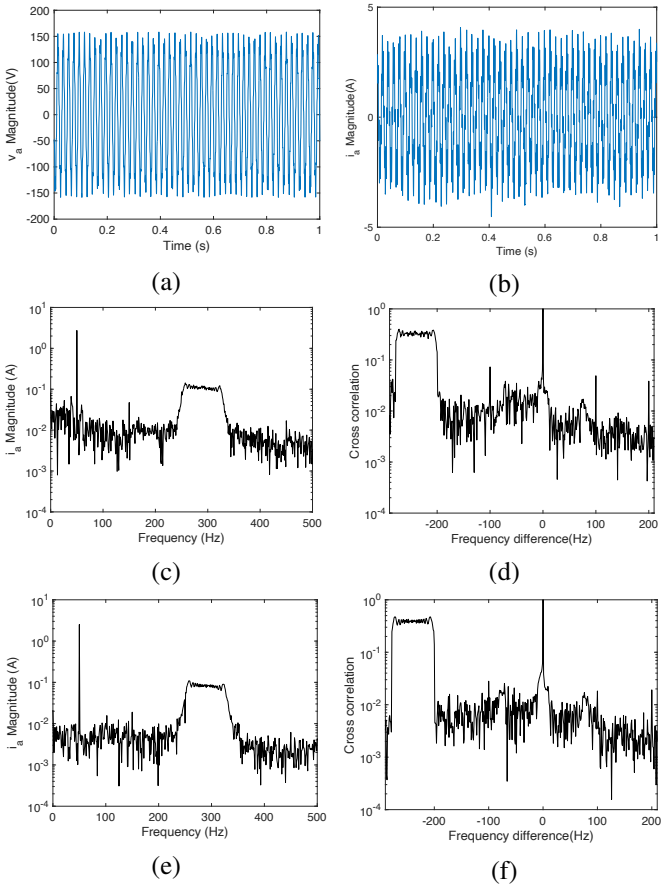

Fig. 6. Experimental results of broken-bar fault detection by injecting a FMCW signal. (a) Time-domain motor voltage signal, (b) Time-domain motor current signal, (c)Motor current frequency spectrum of faulty motor, (d) Fault signature analysis result of faulty motor using cross correlation, (e) Motor current frequency spectrum of healthy motor, and (f) Fault signature analysis result of healthy motor using cross correlation.

REFERENCES

[1] P. Zhang, Y. Du, T. G. Habetler, and B. Lu, "A survey of condition monitoring and protection methods for medium-voltage induction motors," *IEEE Transactions on Information Theory*, vol. 47, no. 1, pp. 34–46, 2011.

[2] P. M. Santos, M. B. R. Correa, C. B. Jacobina, E. R. C. da Silva, A. M. N. Lima, G. Didiery, H. Raziky, and T. Lubiny, "A simplified induction machine model to study rotor broken bar effects and for detection," in *Proceedings of the 37th IEEE Power Electronics Specialists Conference(PESC)*, June 2006, pp. 1–7.

[3] F. Filippetti, G. Franceschini, C. Tassoni, and P. Vas, "AI techniques in induction machines diagnosis including the speed ripple effect," *IEEE Transactions on Industry Applications*, vol. 34, no. 1, pp. 98–108, Jan 1998.

[4] B. Xu, L. Sun, L. Xu, and G. Xu, "An ESPRIT-SAA-based detection method for broken rotor bar fault in induction motors," *IEEE Transactions on Energy Conversion*, vol. 27, no. 3, pp. 654–660, Sep 2012.

[5] Y. Kim, Y. Youn, D. Hwang, J. Sun, and D. Kang, "High-resolution parameter estimation method to identify broken rotor bar faults in induction motors," *IEEE Transactions on Industrial Electronics*, vol. 60, no. 9, pp. 4103–4117, Sep 2013.

[6] D. Liu and D. Lu, "Off-the-grid compressive sensing for broken-rotor-bar fault detection in squirrel-cage induction motors," *IFAC-PapersOnLine*, vol. 48, no. 21, pp. 1451–1456, 2015.

[7] F. Briz, M. W. Degner, A. B. Diez, and J. M. Guerrero, "Online diagnostics in inverter-fed induction machines using high-frequency signal injection," *IEEE Transactions on Industry Applications*, vol. 40, no. 4, pp. 1153–1161, 2004.

[8] S.-K. Kim and J.-K. Seok, "High-frequency signal injection-based rotor bar fault detection of inverter-fed induction motors with closed rotor slots," *IEEE Transactions on Industry Applications*, vol. 47, no. 4, pp. 1624–1631, 2011.

[9] J. Cusidó, L. Romeral, J. A. Ortega, A. Garcia, and J. Riba, "Signal injection as a fault detection technique," *Sensors*, vol. 11, no. 3, pp. 3356–3380, 2011.

[10] X. Luo, Y. Liao, H. Toliyat, A. El-Antably, and T. A. Lipo, "Multiple coupled circuit modeling of induction machines," in *Conference Record of the 1993 IEEE Industry Applications Society Annual Meeting*, vol. 1, Oct 1993, pp. 203–210.

[11] M. Boucherma, M. Y. Kaikaa, and A. Khezzar, "Park model of squirrel cage induction machine including space harmonics effects," *Journal of Electrical Engineering*, vol. 57, no. 4, pp. 193 – 199, 2006.

[12] D. Liu, R. Sugawara, and P. Orlik, "EMI reduction in PWM inverters using adaptive frequency modulation carriers," in *2020 23rd International Conference on Electrical Machines and Systems (ICEMS)*. IEEE, 2020, pp. 772–777.